

A large rotating structure around AB Doradus A at VLBI scale

J. B. Climent¹ , J. C. Guirado^{1,2}, R. Azulay¹ and J. M. Marcaide¹

¹Departament d'Astronomia i Astrofísica, Universitat de València, C. Dr. Moliner 50,
46100 Burjassot, València, Spain
email: j.bautista.climent@uv.es

²Observatori Astronòmic, Universitat de València, Parc Científic, C. Catedrático
José Beltrán 2, 46980 Paterna, València, Spain

Abstract. We report the results of three VLBI observations of the pre-main-sequence star AB Doradus A at 8.4 GHz. With almost three years between consecutive observations, we found a complex structure at the expected position of this star for all epochs. Maps at epochs 2007 and 2010 show a double core-halo morphology while the 2013 map reveals three emission peaks with separations between 5 and 18 stellar radii. Furthermore, all maps show a clear variation of the source structure within the observing time. We consider a number of hypothesis in order to explain such observations, mainly: magnetic reconnection in loops on the polar cap, a more general loop scenario and a close companion to AB Dor A.

Keywords. stars: pre-main-sequence, stars: rotation, stars: imaging, stars: magnetic fields, stars: flare, radio continuum: stars

1. Introduction

About 15 pc away, AB Doradus is a pre-main-sequence (PMS) system formed by two pairs of stars separated by 9'', AB Dor A/C and AB Dor Ba/Bb (Close *et al.* 2005; Guirado *et al.* 2006), giving name to the AB Doradus moving group (AB Dor-MG). The main star of this system, the K0 dwarf AB Dor A is a PMS star (Herbst & Shevchenko 1999) with a rotation period of 0.5 days and presents strong emission at all wavelengths, from radio to X-rays. It has been well studied by the Hipparcos satellite (Lindgren & Kovalevsky 1995; Lestrade *et al.* 1995) and very-long-baseline-interferometry (VLBI) arrays (Lestrade *et al.* 1995; Guirado *et al.* 1997; Azulay *et al.* 2017). This joined effort revealed the presence of AB Dor C, a low-mass companion with $0.090 M_{\odot}$, orbiting AB Dor A at an average angular distance of $0.2''$. The pair AB Dor A/C has also been observed by different near-infrared instruments at the VLT (Close *et al.* 2005, 2007; Boccaletti *et al.* 2008) allowing independent photometry of AB Dor C which, along with the dynamical mass determination, served as a benchmark for stellar evolutionary models. The exact age of the system is a current subject of discussion: 40–50 Myr for AB Dor A and 25–120 Myr for AB Dor C in Azulay *et al.* (2017), 40–60 Myr in Zuckerman *et al.* (2004) and López-Santiago *et al.* (2006), 30–100 Myr in Close *et al.* (2005), 40–100 Myr in Nielsen *et al.* (2005), 75–150 Myr in Luhman & Potter (2006), 50–100 Myr in Janson *et al.* (2007) and Boccaletti *et al.* (2008), 40–50 Myr in Guirado *et al.* (2011), >110 Myr for the AB Dor nucleus star in Barenfeld *et al.* (2013) and 130–200 Myr in Bell *et al.* (2015).

Here we present a new analysis of the 8.4 GHz VLBI data from Azulay *et al.* (2017) in order to look for more information beyond the astrometric position.

Table 1. Model components of the fit of circular Gaussians on the uv -plane for VLBI observations.

Epoch	Comp. ^a	S (mJy)	θ (mas)	T_b (K)
2007	1	3.4 ± 0.5	1.41 ± 0.18	$4.2 \cdot 10^7$
	2	1.3 ± 0.2	0.60 ± 0.1	$8.9 \cdot 10^7$
2010	1	2.31 ± 0.17	1.30 ± 0.09	$3.4 \cdot 10^7$
	2	1.20 ± 0.16	1.51 ± 0.18	$1.3 \cdot 10^7$
2013	1	2.7 ± 0.2	0.90 ± 0.08	$8.3 \cdot 10^7$
	2	0.80 ± 0.15	0.40 ± 0.07	$1.2 \cdot 10^8$
	3	1.48 ± 0.19	0.65 ± 0.08	$8.7 \cdot 10^7$

Notes. ^aWe adopt the convention that the central component will be denoted by subindex 1. In case of detection, the subindex 2 will indicate the presence of a second component to the east. In 2013, subindex 2 indicates the closest component to the east while subindex 3 the furthest one. S represents the flux density, θ the FWHM diameter of the circular Gaussian component and T_b the minimum brightness temperature.

2. Observations and data reduction

We observed the binary system AB Dor A/C using the Australian Long Baseline Array during 11 November 2007, 25 October 2010 and 16 August 2013 at X band (see Table 1 in [Azulay *et al.* 2017](#)). Each observation lasted 12 hours. The system was observed in phase referencing mode using the ICRF-defining source BL Lac PKS 0516-621 (about 3.6° away) as a phase calibrator. The sequence calibrator-target lasts about 3.5 minutes. Both RCP and LCP polarizations were recorded using four 16 MHz bandwidth subbands per polarization.

We reduced and analyzed the data using the Astronomical Image Processing System (AIPS) of the National Radio Astronomy Observatory (NRAO) with standard routines. Firstly, we calibrated the ionospheric delay and corrected the instrumental phases. We then calibrated the visibility amplitudes using the nominal sensitivity for each antenna and corrected the phases for parallactic angles. Finally, we performed a fringe-search on the phase calibrator to minimize the residual contributions to the phases and applied these new corrections to our target. The phase-referenced channel-averaged images were obtained using the Caltech imaging program DIFMAP ([Shepherd *et al.* 1994](#)) with the clean algorithm while selecting the polarization of interest in each case. The AB Dor A image for each epoch and band is shown at Fig. 1. In addition to producing an image of AB Dor A/C for each LBA dataset, we also fitted circular Gaussians to the interferometric visibilities (uv plane) using the DIFMAP task modelfit (the use of elliptical Gaussians resulted in very small non-physical FWHM values). The fitting results can be found in Table 1.

3. Results

3.1. VLBI Imaging and Model Fitting of AB Dor A

All of our VLBI images of AB Dor A are presented in Fig. 1. As can be appreciate, we found a complex structure in all three epochs. In all cases, the brightest peak of emission is located at the map center, coincident (to within one beam size) with the expected position of AB Dor A according to the kinematics reported in [Azulay *et al.* \(2017\)](#). In 2007 and 2010, two emission peaks or components can be identified, separated by 3.1 ± 0.2 mas ($\sim 10 R_{\text{star}}$) and clearly oriented east-west in both epochs. In the latter epoch, the double point-like structure is not as clearly separated as in 2007 resulting in a double core-halo morphology. Later on, in 2013 the structure becomes even more complex: the pair of brightest peaks (components 1 and 3) are separated by 5.7 ± 0.3 mas ($\sim 18 R_{\text{star}}$)

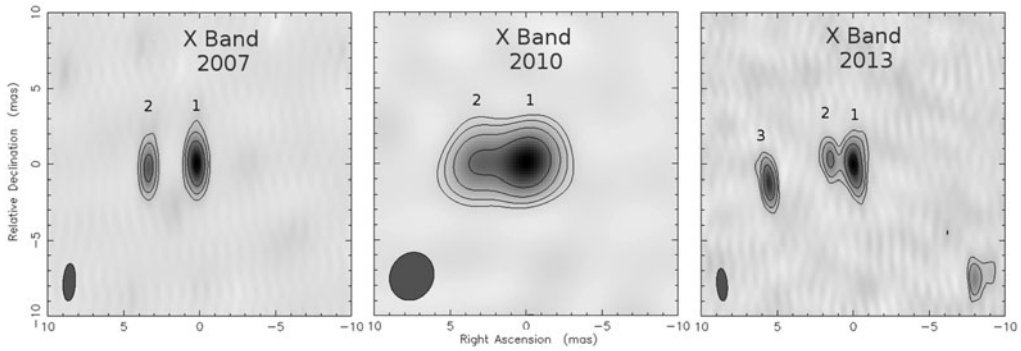


Figure 1. LBA images of all our observations of AB Dor A. Here and hereafter, north is up and east to the left. Numbers (if any) indicate the index assigned to each component. The contour levels, peak brightness and background rms noise for each image are as follows: (2007): 11%, 22%, 44% and 88%, $2.35 \text{ mJy beam}^{-1}$, $0.06 \text{ mJy beam}^{-1}$; (2010): 6%, 12%, 24%, 48%, and 96%, $2.16 \text{ mJy beam}^{-1}$, $0.05 \text{ mJy beam}^{-1}$; (2013): 10%, 20%, 40% and 80%, $1.80 \text{ mJy beam}^{-1}$, $0.05 \text{ mJy beam}^{-1}$. All the images are centered at the expected positions of AB Dor A.

with a component between them (component 2) at $1.6 \pm 0.1 \text{ mas}$ ($\sim 5 R_{\text{star}}$) away from the center. The possible nature of this structure is discussed in Sect. 4; however it is important to notice that, given this complex morphology, the kinematics of AB Dor A might be artificially biased towards the centered peak of the images, not necessarily associated to the photosphere of the star, and not necessarily associated to the same feature for different epochs. Actually, this is likely the limiting factor of the precision of the orbit determination provided for AB Dor A (Azulay *et al.* 2017).

3.2. Time analysis of AB Dor A images

The images shown in Fig. 1 correspond to the structure of AB Dor A obtained with the full interferometric data set extending throughout the complete duration of each observation (typically 10 hr), which actually covers nearly one rotation period of the star ($\sim 12 \text{ hr}$). Therefore these images, and in particular, the complex structures observed at X-band, represent the emission of AB Dor A averaged over the turnaround period of the star.

If the morphology of AB Dor A happens to vary within the duration time of each observation, this will show a dependence of the observed structure with its rotation period. To further investigate this dependence we divided each X-band VLBI observation into two time intervals which allowed us to obtain two “snapshot” images for each epoch (shorter time intervals resulted in very sparse uv coverage and, therefore, maps of degraded quality with unreliable structures). We should emphasize that each snapshot image conserves its own astrometric information (referenced to the external quasar), that is, the snapshot images can be properly registered. As can be seen in Fig. 2, the snapshot maps corresponding to the same observational epoch (but different UT ranges) show remarkable differences. In 2007 and 2010 the snapshot images indicate that the double core-halo morphology is present at both intervals, a feature also visible in the entire data set images. However, the details of the structures change significantly on timescales of a few hours: the easternmost component seems to have rotated between snapshots with respect to the central, brightest emission an angle of $40 \pm 3^\circ$ ($47 \pm 3^\circ$) at epoch 2007 (2010). On the other hand, the distance between the peaks of the components increases (decreases) $0.7 \pm 0.3 \text{ mas}$ ($1.5 \pm 0.4 \text{ mas}$) between snapshots at epoch 2007 (2010). Both epochs start at similar rotational phases of the star: 0.30 for 2007 and 0.39 for 2010.

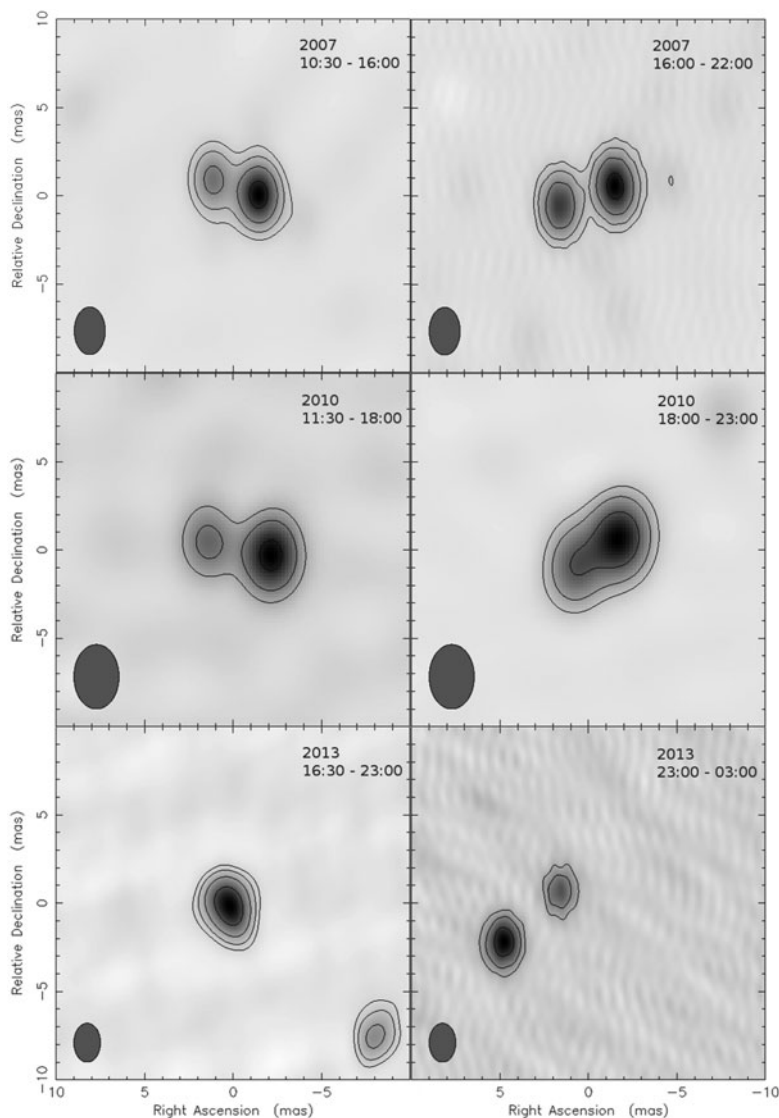


Figure 2. LBA snapshot images of AB Dor A at X band. The left column shows the first half of the observation while the right column the second half. The different epochs are shown in different rows. We have forced both the contour levels and the beam size to be exactly the same during the same epoch, choosing the average of the beam sizes of the observation halves. The FWHM beam size, its orientation, contour levels and coordinates of the map center for each epoch are as follows: **(2007)**: 1.75×2.7 mas at 0° , 10%, 20%, 40% and 80% of $3.01 \text{ mJy beam}^{-1}$, $5:28:44.916066$, $-65:26:53.866084$; **(2010)**: 2.55×3.65 mas at 0° , 15.5%, 31% and 62% of $2.46 \text{ mJy beam}^{-1}$, $5:28:44.943182$, $-65:26:53.454600$; **(2013)**: 1.5×2.2 mas at 0° , 8%, 16%, 32% and 64% of $3.84 \text{ mJy beam}^{-1}$, $5:28:44.964236$, $-65:26:52.995000$.

Finally, the appearance of the snapshots at epoch 2013 (see Figure 2) shows a very different behaviour with a strong time dependence: The first snapshot, corresponding to the first half of the observation, shows a unique central component coincident with the brightness peak found in the maps constructed with the entire data set (named as comp. 1 in Fig. 1). However, somewhat surprisingly, this component 1 is not present in the second snapshot, where only components 2 and 3 are visible. We notice that, as seen in

Table 2. Flux density of the components present in the snapshots (Fig. 2).

Epoch	S_1 (mJy)	S_2 (mJy)
11 Nov. 2007		
10:30-16:00	3.6 ± 0.3	1.1 ± 0.2
16:00-22:00	3.5 ± 0.6	1.5 ± 0.3
25 Oct. 2010		
11:30-18:00	1.8 ± 0.3	0.8 ± 0.3
18:00-23:00	1.7 ± 0.4	1.3 ± 0.4
16 Aug. 2013		
	S_1 (mJy)	S_4 (mJy)
16:30-23:00	5.4 ± 0.3	2.5 ± 1.1
	S_2 (mJy)	S_3 (mJy)
23:00-03:00	1.4 ± 0.2	2.1 ± 0.3

the maps, neither component 2 nor component 3 are spatially coincident with component 1, the latter corresponding to the predicted position by the known orbit of AB Dor A.

Following the same procedure described in Sect. 2, we fitted circular Gaussians to the interferometric visibilities for each time interval (Table 2). Due to the resemblance with the entire data set image and in order to make the comparison easier, we fixed the component sizes to those measured in Table 1. Both in 2007 and 2010, the brightest component flux remains constant during the entire observation while the second component might be slightly increasing in flux during the second half. The total detected flux (sum of the components) decreased a factor 2 from 2007 to 2010. Since the full observation image shows the average flux during the entire time, the 2013 components fluxes as they appear in different time intervals (Table 2) are greater than those measured in the entire data set image (Table 1).

4. Discussion

X-band detections (Fig. 1 and Fig. 2) present a challenge to the “electrons in a closed coronal loop” scenario. Possible explanations will be explored in detail in Climent *et al.* (in prep) and must account for the observed properties:

- A complex internal structure. Not only an explanation for the emission at the expected position of AB Dor A but also for one (2007 and 2010) or two (2013) extra components is needed.
- Extra components located at $5 R_{\text{star}}$, $10 R_{\text{star}}$ and $18 R_{\text{star}}$ away from the central component in east-west direction.
- Variability of the components position on a timescale of hours (see Fig. 2).
- Low degree of circular polarization ($<10\%$) in all the components.
- Brightness temperatures between 10^7 K and 10^8 K in all the components.

Previous studies of Algol (Mutel *et al.* 1998) and UV Ceti found that a strong, large-scale, dipole field could be consistent with the double-lobe structure observed in VLBI images of these objects. In these cases, one emission region would be located above one polar cap of the star while the other emission region would originate in a region above the other polar cap. Our 2007 and 2010 X-band images possess a great morphological resemblance with the double-lobe structure detected in Algol and UV Ceti. Hence, a polar cap model should be fully tested to see if it can properly explain our observations.

A flaring model where two magnetic loop structures are anchored to opposite sides of the star, similarly to what has been proposed for UX Arietis (Franciosini *et al.* 1999) and HR 1099 (Ransom *et al.* 2002), could explain our observations where the detected components would originate near or above the top of such loops where magnetic reconnection events occur. Due to the high frequency of slingshot prominences in AB Dor A, we may

have detected the magnetic reconnection occurring on top of one of these prominences, that is, a helmet streamer similar to the solar ones. Although it is difficult to address this question with the limited data, one month after our 2007 observations, two big slingshot prominences were present in AB Dor A (Jardine, private communication). Although the lifespans of these phenomena are 2–3 days, this might be indicative that this scenario is, at least, plausible.

Although it may be tempting to interpret the X band images (Fig. 1) as a binary system (identifying AB Dor A as component 1 and the companion as component 2), the temporal analysis of Fig. 2 makes this scenario highly unlikely. Assuming that the axis of the orbital plane is parallel to the rotational axis of AB Dor A, at 3 mas separation, the orbital motion of component 2 (in 2007 and 2010) would imply a value of the radial velocity semi-amplitude of the stellar reflex motion much greater than the measured upper limit of $\sim 1 \text{ Km}\cdot\text{s}^{-1}$. Moreover, this hypothesis fails to explain why no motion is detected in component 1 in 2007 while, in 2010, component 1 clearly moves. Finally, this scenario is unable to properly explain the 2013 snapshot images since no companion would be detected during the first half of the observation while AB Dor A would disappear during the second half. For these reasons we conclude that the scenario of a companion to AB Dor A is highly unlikely and unable to reproduce our images.

As previously stated, the details of these hypothesis, how well they explain our observations, and their possible consequences will be further explored in Climent *et al.* (in prep).

References

- Azulay, R., Guirado, J. C., Marcaide, J. M., *et al.* 2017, *A&A*, 607, A10
 Barenfeld, S. A., Bubar, E. J., Mamajek, E. E., & Young, P. A. 2013, *ApJ*, 766, 6
 Bell, C. P. M., Mamajek, E. E., & Naylor, T. 2015, *MNRAS*, 454, 593
 Boccaletti, A., Chauvin, G., Baudoz, P., & Beuzit, J.-L. 2008, *A&A*, 482, 939
 Close, L. M., Lenzen, R., Guirado, J. C., *et al.* 2005, *Nature*, 433, 286
 Close, L. M., Thatte, N., Nielsen, E. L., *et al.* 2007, *ApJ*, 665, 736
 Franciosini, E., Massi, M., Paredes, J. M., & Estalella, R. 1999, *A&A*, 341, 595
 Guirado, J. C., Reynolds, J. E., Lestrade, J.-F., *et al.* 1997, *ApJ*, 490, 835
 Guirado, J. C., Martí-Vidal, I., Marcaide, J. M., *et al.* 2006, *A&A*, 446, 733
 Guirado, J. C., Marcaide, J. M., Martí-Vidal, I., *et al.* 2011, *A&A*, 533, A106
 Herbst, W. & Shevchenko, V. S. 1999, *AJ*, 118, 1043
 Janson, M., Brandner, W., Lenzen, R., *et al.* 2007, *A&A*, 462, 615
 Lindegren, L. & Kovalevsky, J. 1995, *A&A*, 304, 189
 Lestrade, J.-F., Jones, D. L., Preston, R. A., *et al.* 1995, *A&A*, 304, 182
 López-Santiago, J., Montes, D., Crespo-Chacón, I., & Fernández-Figueroa, M. J. 2006, *ApJ*, 643, 1160
 Luhman, K. L. & Potter, D. 2006, *ApJ*, 638, 887
 Mutel, R. L., Molnar, L. A., Waltman, E. B., & Ghigo, F. D. 1998, *ApJ*, 507, 371
 Nielsen, E. L., Close, L. M., Guirado, J. C., *et al.* 2005, *Astron. Nachr.*, 326, 1033
 Ransom, R. R., Bartel, N., Bietenholz, M. F., *et al.* 2002, *ApJ*, 572, 487
 Shepherd, M. C., Pearson, T. J., & Taylor, G. B. 1994, *BAAS*, 26, 987
 Zuckerman, B., Song, I., & Bessell, M. S. 2004, *ApJ*, 613, L65